Stratospheric ozone trends for 1985–2018: sensitivity to recent large variability

William T. Ball[1,2], Justin Alsing[3,4], Johannes Staehelin[1], Sean M. Davis[5], Lucien Froidevaux[6], and Thomas Peter[1]

[1]Institute for Atmospheric and Climate Science, Swiss Federal Institute of Technology Zurich, Universitaetstrasse 16, CHN, CH-8092 Zurich, Switzerland
[2]Physikalisch-Meteorologisches Observatorium Davos World Radiation Centre, Dorfstrasse 33, 7260 Davos Dorf, Switzerland
[3]Oskar Klein Centre for Cosmoparticle Physics, Stockholm University, Stockholm SE-106 91, Sweden
[4]Physics Department, Blackett Laboratory, Imperial College London, SW7 2AZ, UK
[5]NOAA Earth System Research Laboratory Chemical Sciences Division, Boulder, CO, USA
[6]Jet Propulsion Laboratory, California Institute of Technology, Pasadena, CA, USA

Correspondence to: W. T. Ball (william.ball@env.ethz.ch)

Atmospheric
Chemistry
and Physics
Discussions

Abstract. The Montreal Protocol has successfully prevented catastrophic losses of stratospheric ozone, and signs of recovery are now evident. Nevertheless, recent work suggests that ozone in the lower stratosphere (<24 km) continued to decline over 1998–2016, offsetting recovery at higher altitudes and preventing a statistically significant increase in quasi-global (60°S – 60°N) total column

5   ozone. In 2017, a large lower stratospheric ozone resurgence over less than 12 months was estimated (using a chemistry-transport model; CTM) to have wiped out the long-term decline in the quasi-global integrated lower stratospheric ozone column. Here, we extend the analysis of space-based ozone observations to December 2018 using the $BASIC_{SG}$ ozone composite. We find that the observed 2017 resurgence was only around half that modelled by the CTM, was of comparable

10 magnitude to other strong inter-annual changes in the past, and restricted to southern hemispheric mid-latitudes (SH; 60°S–30°S). In the SH mid-latitude lower stratosphere, the data suggest that by the end of 2018 ozone is still likely lower than in 1998 (probability ~80%). In contrast, tropical and northern hemisphere (NH) ozone continue to display ongoing decreases, exceeding 90% probability. Robust tropical (>95%, 30°S–30°N) decreases dominate the quasi-global integrated decrease (99%

15 probability); the integrated tropical stratospheric column (1–100 hPa, 30°S–30°N) displays a significant overall decrease, with 95% probability. These decreases do not reveal an inefficacy of the Montreal Protocol. Rather, they suggest other effects to be at work, mainly dynamical variability on long or short timescales, counteracting the protocol's regulation of halogenated ozone depleting substances (hODS). We demonstrate that large inter-annual mid-latitude variations (30°–60°),

20 such as the 2017 resurgence, are driven by non-linear QBO phase-dependent seasonal variability. However, this variability is not represented in current regression analyses. To understand if observed lower stratospheric decreases are a transient or long-term phenomenon, progress needs to be made in accounting for this dynamically-driven variability.

1   Introduction

25 Ozone in the stratosphere acts as a protective shield against ultraviolet radiation that may harm the biosphere, and leads to cataracts, skin damage, and skin cancer in humans (Slaper et al., 1996; WMO, 2014, 2018). In the latter half of the 20th century, the emission of long-lived halogen-containing ozone depleting substance (hODSs) led to ~5% loss in quasi-global (60°S–60°N) integrated total column ozone (WMO, 2014), which represents the combined changes in tropospheric and strato-

30 spheric ozone contributions. The 1987 Montreal Protocol and its amendments led to a reduction in hODSs that coincided with a halt in total column ozone losses around 1998–2000 (Harris et al., 2015; Chipperfield et al., 2017).

However, there is still no evidence of a significant increase in total column ozone since 1998 (Chipperfield et al., 2017; Weber et al., 2017; Ball et al., 2018), despite a significant increase in

35 upper stratospheric ozone (1–10 hPa) (Ball et al., 2017; Steinbrecht et al., 2017; Ball et al., 2018;

Petropavlovskikh et al., 2019). Ball et al. (2018) and Ziemke et al. (2018) presented evidence, using OMI/MLS tropospheric column observations for 2005–2016, that tropospheric ozone had also increased significantly. However, large uncertainties remain in quasi-global tropospheric ozone trends, and the recent Tropospheric Ozone Assessment Report (TOAR) shows that different tropospheric

40 ozone products give a wide range of trends, some even indicating negative changes (Gaudel et al., 2018). If tropospheric and upper stratospheric ozone have indeed both increased, then the observed flat trend in total column ozone implies that middle and lower stratospheric ozone should have decreased.

To assess trends in stratospheric ozone, composites must be formed by merging multiple ozone

45 timeseries into a long, multi-decadal record from which variability can be attributed, and long-term trends determined. Composites are subject to artefacts from merging different observing platforms. Multiple papers (Tummon et al., 2015; Harris et al., 2015; Steinbrecht et al., 2017; Ball et al., 2017, 2018) and a SPARC report (Petropavlovskikh et al., 2019) review, discuss, and attempt to account for the artefacts in the uncertainty budget.

50 Ball et al. (2018) integrated ozone over the whole stratosphere, i.e. the ozone layer, quasi-globally for pressure levels from 147–1 hPa (~13–48 km) at mid-latitudes (30°–60°), and 100–1 hPa (~16–48 km) between the sub-tropics (30°S–30°N), and found ozone to be lower in 2016 than in 1998 in multiple ozone composites. In their analysis, the lower stratosphere (147/100–32 hPa, ~13/17–24 km) was driving this decrease. The most significant decreases were in the tropics, but negative

55 trends extended out into the mid-latitudes (Fig. 1d). Other studies have subsequently confirmed these negative trends (Zerefos et al., 2018; Wargan et al., 2018; Chipperfield et al., 2018). Evidence points towards dynamical variations driving changes (Chipperfield et al., 2018), perhaps in the form of enhanced isentropic mixing (Wargan et al., 2018). Although the underlying driving force has not yet been determined, climate change is an obvious, though unverified candidate (Ball et al., 2018).

60 On the other hand, Stone et al. (2018) showed that negative trends could be simulated in the lower stratosphere over the same period in two of nine ensemble members of a coupled chemistry climate model (CCM) as a result of natural variability interfering in the (linear) trend analysis; they suggested that an additional seven years of observations would lead to the negative signal disappearing in favour of positive trends. The implication is then that the observed negative trend over the relatively short

65 19 year timeframe may be a temporary result from large natural variability (in the single realisation) of the real-world, rather than forced by climate-change.

Chipperfield et al. (2018) used a chemistry transport model (CTM) to reconstruct ozone variability close to past real-world behaviour; dynamics in the CTM are driven by ERA-Interim (Dee et al., 2011) reanalysis fields together with a chemistry module. The results showed changes similar to

70 those presented by Ball et al. (2018) up to December 2016. They extended their CTM analysis by an additional 12 months to find that the 1998–2016 decline in the lower stratosphere (~2 DU; Ball et al. (2018)) was wiped out by a sudden increase of ozone in 2017, exceeding 8 DU quasi-globally.
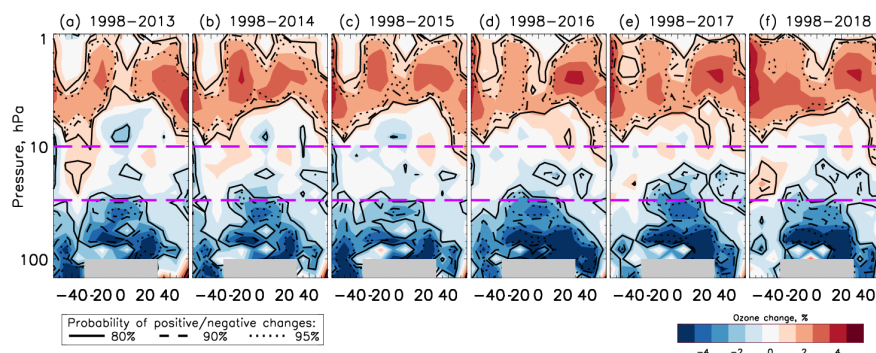
Atmospheric
Chemistry
and Physics
Discussions

Figure 1: Zonally averaged ozone change between 1998 and end years (a) 2013 to (f) 2018. Red represents increases, blue decreases (%; right legend). Contours represent probability levels of positive or negative changes (left legend). Grey-shaded regions represent unavailable data. Pink dashed-lines delimit regions integrated to partial ozone columns in other figures.

This was attributed almost entirely to dynamical changes and was primarily located in the southern hemisphere. They suggested that the lower stratospheric ozone decrease was a result of large natural

75   variability that biased the trend analysis, and that the variability could be attributed to dynamics and not to chemical or photolytic changes, although the source of dynamical perturbations was not identified or the impact on trends quantified.

Here, we update the observational analysis of Ball et al. (2018) to include data to the end of 2018 (Section 3.1). This allows us to assess the impact of the 2017 ozone increase in the lower

80   stratosphere on the trend analysis, and to consider additional changes over 2018. We show that large ozone-increase events, with a duration and magnitude similar to that of 2017 (Chipperfield et al., 2018) have occurred regularly since 1985 at mid-latitudes (Section 3.2), and find the events are linked to a seasonally-dependent QBO effect (Section 3.3). We update partial column ozone trends from 2016 to 2018 in section 3.4. Finally, we consider the sensitivity of trends to the recent

85   increase of stratospheric ozone (Sections 3.5-3.6) by considering six periods that start in 1985 and end between 2013 and 2018, in order to demonstrate where signals are robust to the end date, and where not. Such an analysis is essential to establish if the negative trends are a result of natural variability interfering in the trend analysis, and to take the first steps to account for what may be driving the large, short-term variability.

2 Data and methods

2.1 Ozone Data

Although other ozone composites exist (Petropavlovskikh et al., 2019), we focus exclusively on data formed from merging ozone from SWOOSH (Davis et al., 2016) and GOZCARDS (see Froidevaux et al. (2015), but here we use the updated v2.20 – see Froidevaux et al. (in review, 2018)) using the so-called BASIC (BAyeSian Integrated and Consolidated) approach (Ball et al., 2017) to account for artefacts in merged composites and improve trend estimates. This data was referred to as 'Merged-SWOOSH/GOZCARDS' by Ball et al. (2018), but we refer here to it as $BASIC_{SG}$. To briefly place the SWOOSH and GOZCARDS datasets in context of $BASIC_{SG}$, Figure S1 of Ball et al. (2018) presented 1998–2016 changes using SWOOSH or GOZCARDS alone; this figure reveals that these ozone composites show generally similar changes on large spatial scales, though there are clear differences on small scales, e.g. in the tropical upper stratosphere, and in the southern hemisphere lower stratosphere. Figure S2 of Ball et al. (2018) importantly demonstrates at 100 hPa in the tropical lower stratosphere that there are significant differences between SWOOSH and GOZCARDS in the late 1990s; this figure also shows that $BASIC_{SG}$ is able to account for the differences in a principled way that is not simply the averaging the two products, which is particularly important for having confidence in an assessment of the lower stratosphere. We extend $BASIC_{SG}$ from Ball et al. (2018) by two years to cover 1985–2018. This period is essentially an extension of the Aura Microwave Limb Sounder (Aura/MLS); both SWOOSH and GOZCARDS consider Aura/MLS exclusively after 2009.

We only consider $BASIC_{SG}$ here for the following reasons. First, as discussed in Ball et al. (2018), compared to the other composites it had the least apparent artefacts within the timeseries. The Stratosphere-troposphere Processes And their Role in Climate (SPARC) Long-term Ozone Trends and Uncertainties in the Stratosphere (LOTUS) report (Petropavlovskikh et al., 2019) indicates this method to be more robust to outliers than other composites. Second, $BASIC_{SG}$ is resolved in the lower stratosphere, which is not the case for all composites; for further discussion see Ball et al. (2018) and the SPARC LOTUS report (Petropavlovskikh et al., 2019). Additionally, SWOOSH and GOZCARDS are currently two of the most up-to-date composites available. Finally, we are interested here in the sensitivity of stratospheric ozone changes to different end years and, since Aura/MLS is arguably one of the best remote sensing platforms for ozone currently in operation (Petropavlovskikh et al., 2019), focusing only on $BASIC_{SG}$ provides an analysis, discussion, and interpretation that is free from the complications of considering multiple composites that have multivariate reasons for displaying different behaviour.

Atmospheric
Chemistry
and Physics
Discussions

2.2 Regression analysis

As in Ball et al. (2018), we perform all timeseries analysis using dynamical linear modelling (DLM)
(Laine et al., 2014); we point the reader to Laine et al. (2014) for details on this method and pro-
vide a short overview here. We use the public DLM code DLMMC (available at https://github.com/
justinalsing/dlmmc).

Our DLM approach models the ozone time-series as a (dynamical) linear combination of the fol-
lowing components: two seasonal components (with 6- and 12-month periods respectively), a set
of regressor variables (i.e., proxy time-series describing various known drivers), an auto-regressive
(AR) process, and a smooth non-linear (non-parametric) background trend. DLM differs from tra-
ditional multiple linear regression (MLR) approaches in a number of key ways. Firstly, while MLR
fits for a fixed (constant-in-time) linear combination of seasonal, regressor, and trend components,
DLM can allow the amplitudes of the various components to vary dynamically in time, capturing
richer phenomenology in the data. Here, we allow the amplitude and phase of the seasonal com-
ponents to be dynamic, but keep the regressor amplitudes constant in time; we leave investigation
of more flexible DLM models with dynamic regressor amplitudes to future work. Secondly, MLR
typically assumes a fixed prescription for the shape of the background trend, e.g., a piecewise-linear
or independent-linear trend with some fixed, pre-chosen inflection-date. These assumptions are both
restrictive and give a poor representation of the smooth background trends we expect from nature.
DLM addresses this by instead modelling the trend as a smooth, non-parametric, non-linear curve,
where the 'smoothness' of the trend is controlled by a free parameter that is included in the fit (see
supplementary materials Fig. S1). Thirdly, in practice MLR is often performed by first subtracting
an estimated mean seasonal cycle, fitting the trend and regressor variables to the anomalies, and
then making a post-hoc correction for auto-regressive residuals. This procedure typically does not
propagate the errors on the seasonal cycle and AR parameters in a rigorous way, leading to misrep-
resentation of uncertainties. DLM addresses this by inferring all components of the model simul-
taneously, and formally marginalizing over the uncertainties in all other parameters when reporting
uncertainties on e.g., the trend. We use the same prior assumptions as described in Ball et al. (2018).

Probabilities of an overall increase (decline) in ozone between two dates (Figs. 1, 7, and Table 1)
are computed as the fraction of MCMC samples that show positive (negative) change. Credible
intervals (Figs. 6, 8, 9) are computed as the central 95 and 99 percentiles of the MCMC samples.
The use of 'confidence' or 'significance' is used in this paper interchangeably with 'probability'
and refers specifically to Bayesian probabilities; it does not refer to the application of frequentist
significance tests and/or confidence intervals.

We use the same regressors as Ball et al. (2018): solar (30 cm radio flux, F30) (Dudok de Wit et al.,
2014)), volcanic (latitudinally resolved stratospheric aerosol optical depth, SAOD) (Thomason et al.,
2017), El Niño Southern Oscillation (ENSO) (NCAR, 2013), and the Quasi-Biennial Oscillation,

QBO, at 30 and 50 hPa [1]. In previous analyses, we considered the Arctic and Antarctic Oscillation,
160 AO/AAO [2], as proxies for Northern and Southern surface pressure variability only for partial column
ozone analysis in their respective hemisphere; here we also consider them for the spatially-resolved
analysis and in all cases use both AO and AAO simultaneously – they have little affect outside their
respective regions, but we do not limit the possibility they may influence some variability in either
hemisphere (Tachibana et al., 2018). We use a first order autoregressive (AR1) process (Tiao et al.,
165 1990) to consider auto-correlation in the residuals. We remove a three year period following the
Pinatubo eruption, i.e. June 1991 to May 1994, which is a year longer than the previous analysis, to
avoid any effects of the eruptions that may have persisted. Another key point regarding the SAOD
proxy is that, unlike the other proxies that have been fully updated to the end of 2018 for this
analysis, the SAOD is not available beyond 2016, so we repeat the year 2016 for 2017 and 2018;
170 if any deviations in the SAOD occurred during this period, our analysis will not account for this.
Nevertheless, as can be seen in Fig. 1d here, in comparison to Fig. 1b of Ball et al. (2018), all of
these adjustments to the procedure from Ball et al. (2018) have little impact on the estimated mean
changes in ozone.

3 Results

3.1 Stratospheric ozone changes since 1998

Figure 1d shows the pressure-latitude, spatially-resolved 1998–2016 ozone change, reproducing
Fig. 1b of Ball et al. (2018). Minor differences exist because the BASIC$_{SG}$ composite has been
updated. Ozone in the lower stratosphere (delimited by the pink dashed line at 32 hPa, 24 km) shows
a marked and almost hemisphere-symmetric decrease, while upper stratospheric changes (>10 hPa,
180 32 km) are mainly positive; the middle stratosphere generally shows relatively flat trends since 1998
with low probability of an overall change.

Figures 1e and f show the 1998–2017 and –2018 ozone changes, respectively. Four points of interest emerge from the comparison to 1998–2016: (i) while still negative, the magnitude of the lower
stratospheric SH (60°S–30°S) decrease has become smaller and less significant (~80% probability);
185 (ii) tropical (30°S–30°N) and NH (30°N–50°N) changes remain negative and highly probable; (iii)
the probability (and magnitude) of negative trends over tropical and NH regions in the middle stratosphere (32–10 hPa) has increased; and (iv) the magnitude and probability of upper stratospheric
recovery has strengthened. Importantly, Fig. 1 demonstrates the robustness of negative trends in the
lower and positive trends in the upper stratosphere, irrespective of the final year of the analysis. Figures 1a–f present ozone changes from 1998 to end years 2013 through 2018, showing the sensitivity
190 of ozone trends to six consecutive end years. These end years give insight into the sensitivity of the

---

[1]QBO indicies: http://www.geo.fu-berlin.de/met/ag/strat/produkte/qbo/
[2]AO/AAO indicies: http://www.cpc.ncep.noaa.gov/products/precip/CWlink/

Atmospheric
Chemistry
and Physics
Discussions
Open Access
EGU

trends to large inter-annual variability. In particular, these six years encompass periods of both neg-ative/Easterly and positive/Westerly phases of ENSO/QBO. These modes are major contributors to stratospheric variability (Zerefos et al., 1992; Tweedy et al., 2017; Toihir et al., 2018; Garfinkel et al.,

195   2018), and any sensitivity of the end year to the state of these drivers should be encapsulated in this group of spatial responses, particularly if these modes were not well-captured by DLM predictors (Fig. 1). A lower stratosphere negative trend is persistent for all end years. For 1998–2013, there is a highly probable negative trend in the SH lower stratosphere; the probability is retained until 2016, after which it reduces. The opposite is seen in the NH, where only a small region of probable ozone

200   decrease exists for 1998–2013, and this strengthens with each panel until 2016, after which a highly probable decrease remains stable. There is no apparent switch from negative to positive changes in these regions for any of the six end years.

The reduced probability of a SH decrease is related, as we will see in Section 3.2, to the rapid 2017 increase reported by Chipperfield et al. (2018) using a CTM. However, Fig. 1 also confirms

205   in observations that this is localised to south of 30°S and does not reveal coherent or consistent behaviour over time with the NH, suggesting that there may be large, hemispherically independent variability interfering with the trend estimates. Nevertheless, there are no signs as yet of an ozone increase underway in the quasi-global lower stratosphere.

Further, the decrease in ozone in the tropical lower stratosphere increases in magnitude and signif-

210   icance as more data is added. The tropical lower stratospheric ozone is projected to decrease by the end of the century in all chemistry climate models (CCMs) (Dhomse et al., 2018), due to enhanced upwelling of the Brewer Dobson circulation (BDC) resulting from climate change (Polvani et al., 2018). It is possible that this is a detection of the expected tropical lower stratosphere decline in ozone, earlier than expected (WMO, 2014). However, whilst the data show a significant decline, it

215   remains to be seen if this can be attributed to the climate change induced upwelling of the BDC.

3.2 On the rapid increase in ozone in 2017

Chipperfield et al. (2018) reported a rapid increase in the quasi-global lower stratospheric ozone in 2017, modelled using a CTM driven by ERA-Interim reanalysis to represent dynamical vari-ability closer to that which occurred historically. The quasi-global, deseasonalised timeseries from

220   BASIC$_{SG}$ is shown in Fig. 2a; 2017 is bounded by the vertical dashed lines and the large increase is highlighted in red from a minimum in November 2016 to a maximum reached 12 months later in October 2017.

The observed 2016–2017 increase in Fig. 2a was 5.5 DU, which is 63% of the 8.7 DU increase reported by Chipperfield et al. (2018). Split into three latitude bands, 60°–30°S, 30°S–30°N, and

225   30°–60°N (Figs. 2b–d), we find that the upswing can be decomposed into a 12 DU increase in the SH, 3 DU in the tropics, and 6 DU in the NH. Weighting for latitude – 21, 58, and 21% respectively – the SH contribution accounts for nearly half of the quasi-global increase (2.5 DU, 1.9 DU, 1.3 DU).
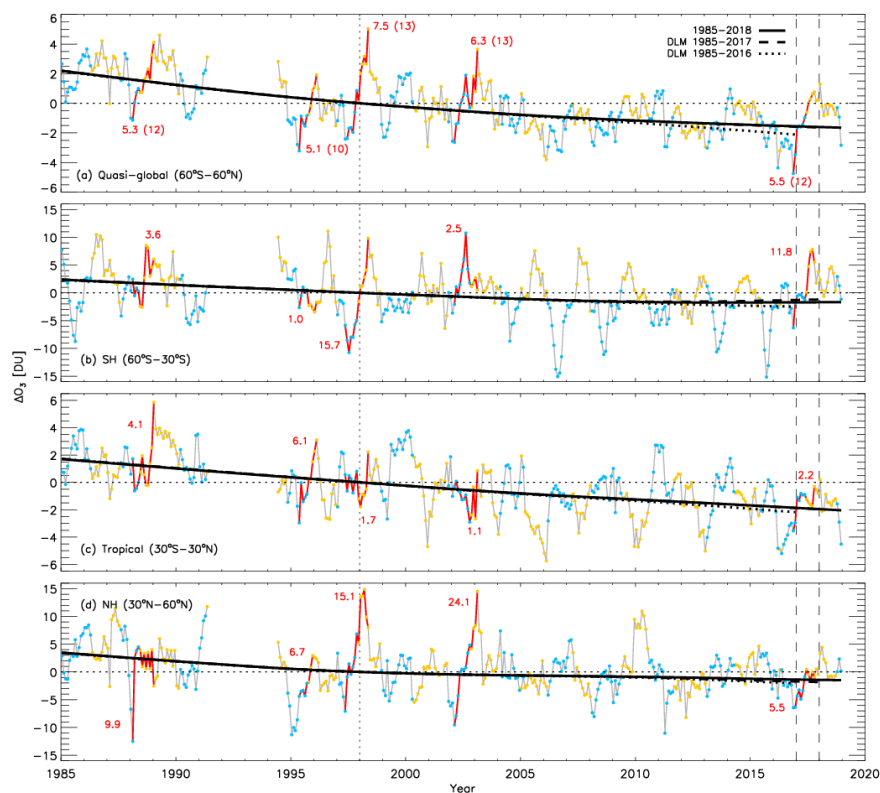
Figure 2: Lower stratospheric partial column ozone anomalies, (a) quasi-global (60°S–60°N), (b) southern hemisphere (60°S–30°S, 147–30 hPa), (c) tropics (30°S–30°N, 100–30 hPa), (d) northern hemisphere (30°N–60°N, 147–30 hPa). The DLM non-linear trend is shown for 1985–2016 (dotted), 1985–2017 (dashed), and 1985–2018 (solid). Red lines represent contiguous periods identified in the quasi-global anomalies exceeding 90% of the magnitude of the November 2016 to October 2017 change within a 13 month period; the DU changes are written above or below each period with period length in brackets; red periods in (b–d) are those identified in (a). Colour dots are plotted on each timeseries when the QBO at 30 hPa is either in an Easterly (yellow) or Westerly (blue) phase. The three-year period following the eruption of Mt. Pinatubo, June 1991 to May 1993, has been removed. Figures for the whole, upper and middle stratosphere are provided in the Supplementary Materials Figs. S2–4.

The overall increase is composed of two sub-periods, dominated by a NH increase until May 2017, and a SH increase over April–August 2017; the tropical region saw comparatively little change in
230 the second period.

Importantly, the rapid increase seen in 2017 is not unique. Four other quasi-global 'events' of this type are found over 1985–2018, shown in Fig. 2a; the identification criteria was an increase of at least 90% of the 2017 increase occurring within a 13 month period. The decomposed timeseries (Fig. 2b–d) show that the large increases in the SH are *normal*, occurring regularly. They also occur

235   in the NH, but not as regularly, and the tropical variability is much smaller than the mid-latitude variance. In addition to the large increases, there are also comparatively large negative swings in both SH and NH timeseries – one in the NH beginning in 2002 exceeds 24 DU. In the following section we argue that these large, rapid changes are driven by a non-linear seasonal-QBO effect.

3.3   Contribution of QBO to mid-latitude ozone variability

240   Chipperfield et al. (2018) convincingly showed that the majority of post-1997 quasi-global ozone variability in Fig. 2a was dynamically controlled. Given that the contributions from each sub-region (Fig. 2b–d) add up to the quasi-global change in 2017, it is reasonable to assume that dynamics controls much of the sub-decadal variability there too. The peaks (or troughs) in the SH are 2–3 years apart; the QBO has a similar periodicity and is known to have the largest inter-annual dynamical

245   impact on ozone in the stratosphere (see Toihir et al. (2018) and Zerefos et al. (1992), and references therein) . Labelling each month in Fig. 2 with the 30 hPa QBO-Easterly or Westerly phase in yellow or blue dots, respectively, reveals that the large SH negative anomalies are almost always associated with a Westerly phase, while positive anomalies are associated with an Easterly phase. This also appears to be the case in the NH, but the variability is less regular, unsurprisingly since the NH

250   stratosphere is known to have additional variability from other drivers. Equatorial variability related to the QBO phase at 30 hPa shows the opposite behaviour to that of the mid-latitudes: decreases generally appear to occur with the Easterly phase and vice versa, and the return from maximum excursion (i.e. the sign of the gradient) appears to be more related to the change in phase.

Histograms of the ozone anomalies relative to the DLM trend line for each QBO phase at 30 hPa

255   are shown in the upper row of Fig. 3. The shift in the histogram between QBO phases is clear in the SH; the NH displays little shift, again likely related to other drivers influencing NH ozone changes, though the extremes show a similar phase separation as in the SH. The difference between the QBO Easterly and Westerly histograms are shown in the bottom row, and make clear the correlation between QBO state and ozone anomalies.

260   To clarify this further, in Fig. 4 all 34 years in the 1985–2018 period are split into 13-month periods starting in January for the SH (upper row) and July for the NH (lower row), i.e. a few month prior to the onset of winter in the respective hemisphere; the latitudes plotted are refined to isolate clearer signals for (a) 50°–30°S, (c) 30°–50°N, and (b,d) 10°S–10°N. This refinement reduces the influence of polar variability on the 30°–50° band, and isolates the equatorial region to where the

265   QBO variability is strongest; we note that the act of forming partial columns of ozone may reduce the integrated variability compared to counter-varying layers that would otherwise be resolved by
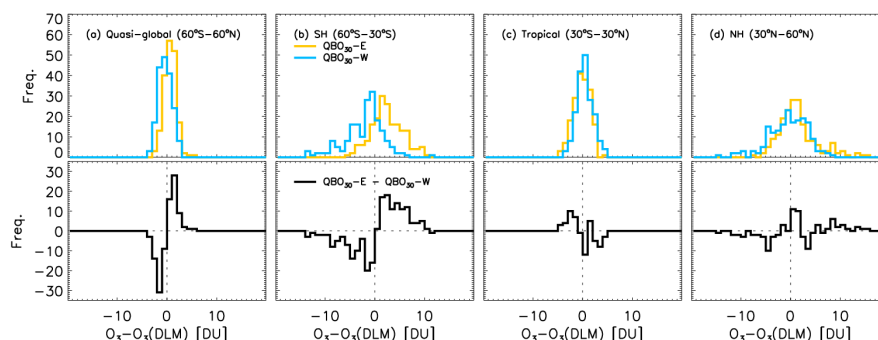
Figure 3: (**Upper row**) Histograms of ozone anomalies relative to the DLM non-linear trend line in Fig. 2 for months when the QBO at 30 hPa is either in an Easterly (yellow) or Westerly (blue) phase: (a) quasi-global (60°S–60°N), (b) southern hemisphere (60°–30°S, 147–30 hPa), (c) tropics (30°S–30°N, 100–30 hPa), (d) northern hemisphere (30°–60°N, 147–30 hPa). (**Lower row** Difference between QBO Easterly and Westerly histograms from the upper row.

pressure level. We find the use of the QBO phase at 70 hPa also better separates the events in this additional analysis. We find negative and positive excursions in the lower stratosphere become clear in 13-month segments when they are bias-shifted to zero in March (a,b) and September (c,d) and

270   then colour coded according to their QBO phase in April or October, respectively (vertical dotted line). The largest deviations are found to occur four months latter (vertical dashed line), at the onset of hemispheric autumn (Holton and Tan, 1980; Dunkerton and Baldwin, 1991).

Once again, the separation of excursions from the mean is clearest for the SH (Fig. 4a) and the corresponding, opposing, equatorial changes (Fig. 4b). The anti-correlated behaviour of excursions

275   between mid-latitude and equatorial regions is consistent with previous studies investigating the relationship between the QBO and mid-latitude ozone variability (Zerefos et al., 1992; Randel et al., 1999; Strahan et al., 2015). We summarise the dynamical concept, in context of these results, in the following (see Baldwin et al. (2001) and Choi et al. (2002) for detailed discussion). The QBO consists of downward propagating equatorial zonal winds; in the lower stratosphere this consists of

280   a Westerly above an Easterly, or vice versa. For Westerly above Easterly (i.e. the 70 hPa QBO is Easterly and lines identified as yellow in Fig. 4): a positive temperature anomaly forms between from sinking air (Fig. 1 of Choi et al. (2002)) that results in increased ozone; a negative temperature anomaly below the Easterly coincides with rising air, and ozone decreases; an equator-to-mid-latitude circulation forms (Randel et al., 1999; Polvani et al., 2010). At mid-latitudes, the return of

285   this meridional circulation draws ozone-rich air from above down into ozone poor regions, anomalously enhancing ozone (yellow, Fig. 4a,c). When Easterlies lie over Westerlies (blue, Fig. 4), the opposite circulation is set up, and ozone anomalies reverse.
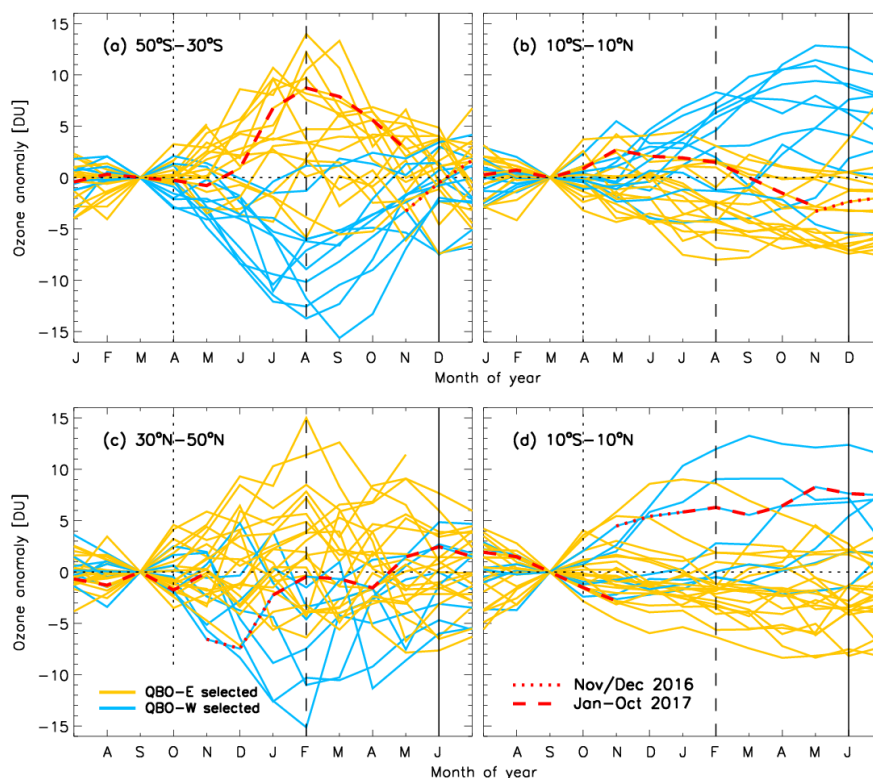
Figure 4: Lower stratospheric partial column ozone at (a) 50°–30°S, (b,d) 10°S–10°N, and (c) 30°–50°N. Each line represents a 13 month period starting in January (upper row) or July (lower row), all bias-shifted to zero in month 3 (March, upper) or 9 (July, lower) and colour coded by the state of the QBO at 70 hPa in month 4 (April, upper) or 10 (August, lower) so that QBO Easterly phases are yellow and Westerly blue. The period covering November to December 2016 is highlighted as a dotted-red line, while January to November is dashed-red.

The 2017 increase is highlighted in Fig. 4, with November 2016 to January 2017 shown as a dotted red line, and January to October 2017 as a red dashed line. Focusing on Fig. 4a in the SH, the increase onset during the Easterly phase is large, but as noted earlier larger excursions have occurred before and regularly (Fig. 2). A prolonged Westerly phase, following the breakdown of the expected QBO pattern in 2016 (Osprey et al., 2016; Newman et al., 2016; Tweedy et al., 2017), may have contributed to a suppressed level of ozone in 2016 (note the single orange dot in 2016 in Fig. 2a signifying a brief Easterly QBO phase). The arrival of the Easterly phase proper in 2017 led to the ozone increase at mid-latitudes. The Westerly phase at 30 hPa began in late 2018 and ozone should,

Atmospheric
Chemistry
and Physics
Discussions

Table 1: Absolute change between 1998 and 2018 in Dobson Units, and probability of a positive or negative change in ozone (%) for integrated regions of the stratosphere. Blue text indicates ozone changes are negative, while red indicate positive changes; bold text indicates probabilities exceeding 90%.

Region	60°–30°S	50°–30°S	30°S–30°N	20°S–20°N	30°–50°N	30°–60°N	50°S–50°N	60°S–60°N
Whole	-0.5 (57)	-0.4 (56)	**-1.9 (95)**	**-2.5 (95)**	-3.2 (83)	-2.6 (77)	-1.1 (86)	-1.1 (86)
Upper	**+0.8 (100)**	**+0.8 (99)**	**+0.7 (96)**	+0.6 (85)	**+0.6 (92)**	**+0.6 (96)**	**+0.8 (100)**	**+0.8 (100)**
Middle	+0.7 (78)	+0.8 (78)	**-0.7 (94)**	**-0.9 (95)**	-0.5 (73)	-0.5 (72)	-0.4 (81)	-0.2 (73)
Lower	-1.6 (80)	-1.7 (82)	**-2.1 (99)**	**-2.1 (98)**	-1.9 (82)	-1.5 (76)	**-1.8 (99)**	**-1.7 (99)**

barring no further QBO breakdown, decrease again in 2019 in the SH mid-latitudes; the last three months of 2018 hint at such a decrease (Fig. 2).

Despite this variability, Fig. 1 indicates that the lower stratospheric negative trends could already be identified throughout the lower stratosphere before, and after, 2016. As such, the QBO breakdown
300 event is likely not the primary cause of the negative trends reported by Ball et al. (2018), but does appear to affect the robustness of the trend depending on the end year. We will investigate this end-year sensitivity in section 3.5.

3.4   Latitude-integrated lower stratospheric trend estimates

While Chipperfield et al. (2018) applied ordinary least squares trend fits to timeseries using a single
305 linear trend, this cannot be compared to multi-variate regression approaches, e.g. DLM and MLR. This is because the former simply asks what the trend in the data is, regardless of the forcing agents, while the latter attempts to separate known (usually quasi-periodic) drivers to distill out the trend that has (usually unknown) drivers of its own. The DLM non-linear trend estimates presented here are the first multivariate analysis applied to ozone timeseries that include the large ozone increase
310 witnessed in 2017. It is important to be clear that long-term trends cannot be compared with single year changes; indeed, the processes governing each other are likely quite different. Whilst large short-term increases will likely bias the whole trend-line for that period under MLR analyses (with piecewise linear and independent linear trends – PWLT or ILT), DLM promises to be more robust in the sense that asymmetric fluctuations will only influence part of the smooth trend over a timescale
315 fixed by the smoothness parameter σ_{trend} that controls how rapidly the trend is allowed to evolve (see Ball et al. (2017) and Fig. S1).

The DLM trends estimated over 1985–2018 in Fig. 2 continue to be negative, monotonic trends up to 2018 in the quasi-global, tropical and NH regions, while the SH trend reaches a minimum in ~2013 before slowly rising. All integrated regions suggest the mean remains below the 1998 level
320 (see Table 1), though the probability of an overall decrease is 99% in the quasi-global, dominated by the tropics (99%), with probabilities of a decrease of 80% and 76% in the SH and NH respectively.

13

Atmospheric
Chemistry
and Physics
Discussions

Except in the SH, monotonic downward trends remain, with the addition of two years only affecting the gradient of the monotonic trends (compare dotted line for the year ending in 2016, with the dashed for 2017 and solid for 2018 in Fig. 2). This agrees with Chipperfield et al. (2018) who

325 suggested the large upswing of 2017 that settled in 2018 affected trends, although this was mainly in the SH. However, it has done little to reduce the overall probability of a decrease in the quasi-global time-series (99%). Furthermore, the shape of the DLM curve is affected only near the end years, such that the period away from the end-date is relatively insensitive to a change in the end year and becomes 'locked-in'[3]. As years prior to 2010 are essentially unaffected by the addition of 2017 and

330 2018, the data show robustly that lower stratospheric ozone did continue to decrease until at least 2010 in all regions. We speculate that the shift back to a QBO-Westerly phase will again decrease ozone at mid-latitudes in 2019 (which appears to have begun in October 2018, see Fig. 2). If that happens it is therefore possible that the non-linear trend estimates will likely decrease again, with the emergent 2013 minimum seen in Fig. 2b likely to shift to a later date or disappear.

335 **3.5   Sensitivity of DLM trends to the end year and non-linear seasonal-QBO effects**

Since mid-latitude ozone excursions depend on the QBO-seasonal interaction, this is a non-linear mode of variability. Without predictors to represent this non-linear behaviour, linear regression models (including both DLM and MLR) cannot capture these excursions and the variability can leak into, and bias, other predictors; most importantly, this may include the trend component of the regression

340 model. In this section we examine the magnitude of this effect through a sensitivity analysis of the DLM trends to the end date of the data, both spatially and with partial columns.

Due to the magnitude of the mid-latitude, seasonally-dependent QBO ozone variability on short (two to three year) timescales, ILT or PWLT applied to the relatively short post-1997 time-series will be sensitive to these large swings in ozone. For the smooth DLM trends on the other hand, we expect

345 the last few years of the curve will be primarily affected, with the rest of the trend being stable. We demonstrate the affect on DLM in Fig. 5 where the partial column regions as presented in Ball et al. (2018) are shown for 10° bands, and quasi-globally (right column), over the whole stratospheric column (top), as well as upper, middle and lower. We show DLM curves estimated from six periods that start in 1985 and end in 2013–2018 as in Fig. 1; all curves are bias shifted to zero in 1998.

350 This provides a visualisation of the sensitivity of the non-linear trends to the end year (and hence also the large resurgence in 2017). The uncertainties associated with a change between 1998 and the end year are presented in Fig. 6 with 95% (dark grey shading) and 99% credible intervals. The results specifically for the 1998–2018 change are combined and presented in Fig. 7 as probability distributions, in the same manner as in Fig. 2 of Ball et al. (2018), where blue and red colours

---

[3]In contrast, for MLR analyses, the entire trend-line is impacted by changes in the end year; this is a good example of the inadequacy of using linear trends to describe these data.

355 represent negative and positive changes respectively, and numbers above each distribution are the
probability of the change (fraction of the probability distributions) being negative.

From the panels of Fig. 5, it is clear that the middle-stratosphere exhibits the largest sensitivity to
the end year and uncertainties are consistently large (Fig. 6); quasi-globally the change is negative
for all end years, but does not exceed 95% probability. The upper stratosphere is also sensitive in

360 the tropics (Fig. 5), but has shifted from negative to positive, although always uncertain (Fig. 6);
at mid-latitudes uncertainties are smaller, but there has been a general shift towards more positive
and significant increases, which is more-clearly reflected in the SH and quasi-global estimates. The
evolution of the lower and whole stratospheric non-linear trends mimic each other: south of 30°S,
the end points of the negative changes have quickly increased in 2017 and 2018, though remain neg-

365 ative in the lower stratosphere; at latitudes north of 30°S, the addition of 2017 and 2018 have made
little difference to the monotonic decline; for 50–60°N, while flat, the additional years make little
difference. The quasi-global lower stratosphere continues to exhibit a monotonic decline that is still
highly confident with 99% probability (Fig. 7 and Table 1), and the whole stratosphere continues
to remain lower than in 1998, though this is now with a probability of 86%; these trends are domi-

370 nated by the tropical contribution (58%, latitude weighted) to the quasi-global change, whereas NH
and SH contribute 21% each. Even so, the NH changes do not appear affected by the recent large
seasonally-dependent QBO variability.

Figure 5 also confirms that the non-linear curves are only affected by unmodelled variance in
years close to the end points; changes prior to the last five years are largely unaffected in the partial

375 columns. Indeed, even with the large increase in 2017 in the SH, we see that all trends agree well
prior to 2010; this is true in other panels, e.g. the middle stratosphere and tropical upper stratosphere.
In the upper stratosphere the recovery onset remains robust, but in the SH lower stratosphere the large
increase in 2017 results in the non-linear trend curve having a local minimum emerge around 2013.
As such we can infer that additional data are unlikely to affect the inferred level of ozone in 2013

380 or push the minima to earlier dates, because the affecting end year moves further away with more
data. However, subsequent data might once again push trends to lower levels, e.g. if mid-latitudes
do respond to a Westerly-phase QBO with ozone reducing sharply as it has done in the past (Fig. 4).
We expand the idea of inferring the likely earliest minimum using the DLM with spatially-resolved
data in the Supplementary Materials.

385 **3.6 Update on ozone profiles**

Briefly, in Fig. 8, we provide updated ozone change profiles for 1998–2018 using the standard latitu-
dinal ranges for the SH (60°–35°S), tropical (20°S–20°N), and NH (35°–60°N) (WMO, 2014, 2018;
Steinbrecht et al., 2017; Petropavlovskikh et al., 2019). Fig. 8, also includes 1998–2016 and 1998–
2017 profiles for comparison and shows that, for 1998–2018, confidence in an upper stratospheric

390 recovery is clear for all latitude bands, including the tropics where it has previously remained be-

low the 95% significance levels. The lower stratosphere shows negative changes at almost all levels, though these generally do not exceed a probability of 95%.

Ball et al. (2018), and Fig. 7, indicated that the 50–60° zonal means in both hemispheres show little change in the lower stratosphere in the last 21 years, while the tropical regions out to 30° show

395 a strong decrease. By modifying the latitudinal extent of the profiles slightly, so that mid-latitudes cover 30–50° to exclude, 50–60° and the tropics are widened to 30°S–30°N to include the subtropics, the modified profiles are presented in Fig. 9. This provides some measure of the sensitivity to the latitudinal ranges chosen. Now we see the tropics show close to 95% confidence of an ozone decrease at all tropical lower stratospheric pressure levels, and there is increased confidence of an ozone

400 reduction in the mid-latitude lower stratosphere. Further, the inclusion of higher latitude regions (20–30°) reinforces the tropical upper stratosphere increase. These results once again reinforce the result that only the SH is affected by the 2017 increase (lower stratosphere), that the Montreal Protocol is working (upper stratosphere), and that the decreases in the lower stratosphere at tropical and NH latitudes remain in place, but are not yet fully understood.

405 **4 Conclusions**

Here, we have extended and analysed the BASIC$_{SG}$ stratospheric ozone composite from Ball et al. (2018) by two years to cover 1985–2018. BASIC$_{SG}$ merges two composites, SWOOSH and GOZ-CARDS. We perform a set of sensitivity tests, using dynamical linear modelling (DLM), on the post-1997 trend estimates to understand the impact of a recently reported, large increase in modelled

410 ozone in the lower stratosphere in 2017 (Chipperfield et al., 2018), following almost two decades of persistently decreasing ozone.

The aim of this work is to build confidence in the current evolution of stratospheric ozone, which is essential to assess ozone trends from observations to assess and ensure model projections to the end of the 21st Century are accurate. Chemistry models resolving the stratosphere are the best tools

415 for attribution and long-range studies of ozone, but different types exist: free-running CCMs generate their own model-dependent internal climate and variability; chemistry transport models (CTMs) use wind, temperature and surface pressure fields fully prescribed by reanalyses; and specified-dynamics CCMs (SD-CCMs) use reanalyses to nudge the internally-generated variability of the model closer to the historical variability in the real atmosphere while attempting to retain model dependent processes

420 and internal consistency. CTMs and SD-CCMs can be extremely useful for attributing historical changes in ozone to evolving concentrations of CO_2 and ODSs (Solomon et al., 2016), or the Sun (Ball et al., 2016), by accounting for dynamical variability in observations.

A recent study (Chipperfield et al., 2018) used a CTM to extend ozone timeseries and found lower stratospheric ozone had rapidly increased in 2017 back to 1998 levels; this was attributed

425 to dynamical variability. CTMs can provide insight as to whether the changes might be driven by

Atmospheric
Chemistry
and Physics
Discussions

photochemistry, chemistry, or dynamics. However, because the dynamical fields are prescribed, the CTM cannot provide insight into the underlying dynamical driver of the long-term decreases or the 2017 increase. We show here that the 2017 increase simulated by the CTM (Chipperfield et al., 2018) was more than 60% larger than that observed, and that the 1998-2017 and -2018 (Fig. 1e and

430   f) change remains negative (60°S-60°N), and significant in the tropics and some sub-regions of the NH (Fig. 1f). Neither free-running CCMs (WMO, 2014), nor SD-CCMs (Ball et al., 2018), have so far been demonstrated to accurately reproduce the long-term changes estimated from observations in the lower stratosphere (Fig. 6).

The effect of the ozone increase in 2017 was small and the probability of an overall ozone decrease

435   remains at 99% for 1998–2018. We note that the lower stratospheric trends are dominated by the tropical regions (30°S–30°N) where the decrease is robust to the end year over 2013–2018, with a probability of 99% that it was lower in 2018 than in 1998. Nevertheless, mid-latitudes out to 50°N also indicate that the decrease persists. We also find that the 2017–2018 addition enhances the magnitude of the upper stratospheric ozone recovery, but that the recovery of the quasi-global (60°S–

440   60°N) ozone layer still displays a reduction since 1998, though the confidence in this has reduced from 95% in 2016 (Ball et al., 2018) to 86% in 2018. Given the high probability of a decrease in tropical middle (94%) and lower (99%) stratospheric ozone, the whole tropical stratospheric column indicates a highly probable decrease (95%) over 1998–2018.

In general, uncertainties on changes since 1998 in partial columns have changed little over 2013–

445   2018, a result likely due to the large fraction of unaccounted variance in the standard set of predictors used in regression analysis. Our analysis shows that ozone continued to decrease until a minimum in at least 2013 in the SH, and continues at all latitudes north of 30°S. By comparing the phase of the QBO with large, 2–3 year inter-annual variability at mid-latitudes, the implication is that these large mid-latitude changes are related to the seasonal-dependence of the QBO, i.e. a non-linearity;

450   if true, this could explain why regression models cannot capture this variability, since such non-linear behaviour is not included. The clarification of the origin of these large mid-latitude changes – occurring every few years – is a high priority.

CCMs are consistent in the sign of their projections, although lower stratospheric variability can differ with observations and there is a large spread on their sensitivity to hODSs (Douglass et al.,

455   2012, 2014), and therefore their return dates. CCMs do a good job on many timescales, but due to historically different internal variability, and parametrized sub-grid scale processes and numerical inaccuracies, behaviour in some regions may not be well-reproduced (SPARC/WMO, 2010). It is clear from modelling studies that pre-Montreal Protocol ozone decreases can be attributed to ODS increases (WMO, 2014), and CCMs and CTMs generally reproduce the Antarctic ozone hole well

460   (Solomon et al., 2016). The halt and initial recovery in total column ozone is almost universally reproduced by CCMs (SPARC/WMO, 2010), as is the upper stratospheric recovery. But, trends

since 1998 in the lower stratosphere have not been demonstrated to be simulated in models in the mid-latitudes, most notably in the NH.

Future predictions tend to focus on how stratospheric ozone will evolve under a given global
465 warming scenario; this is important given that the changing climate may impact inter-annual dynamical variability (Osprey et al., 2016; Newman et al., 2016; Tweedy et al., 2017), and changes in the large-scale circulation in the stratosphere is likely to modify future distributions of ozone (Chipperfield et al., 2017). The overall expectations are that ozone levels will return to 1960s levels globally by ~2050, in the Antarctic by 2100, and by ~2030 and ~2050 in Northern and Southern
470 mid-latitudes, respectively, continuing on to a 'super-recovery' (Dhomse et al., 2018; WMO, 2014, 2018). However, it is neither clear whether the recent increase in SH lower stratospheric ozone will remain at higher levels or will reduce again in 2019 as the QBO shifts to a Westerly phase, nor why the NH continues to show a persistent decrease. Nonetheless, we note that the signal is small compared to the (i) large inter-annual variability, (ii) pre-2000 changes induced by ozone deplet-
475 ing substances, and (iii) ozone loses that would have occurred without the Montreal Protocol being enacted.

The ongoing negative trend of ozone in the lower stratospheric component of the total column also continues to pose a problem for global trends in tropospheric ozone. If tropospheric ozone has really increased over the last two decades, and stratospheric ozone was not decreasing or remained flat,
480 then some component of the total column ozone must have been decreasing to balance the budget. Alternatively, it is possible that the solution simply lies in very large observational uncertainties (Harris et al., 2015; Gaudel et al., 2018; Petropavlovskikh et al., 2019) and/or the inadequacies of linear regression techniques to attribute variability and identify trends. In addition to improving merged-observational records, this calls for a community push to improve detection and attribution
485 techniques to solve an issue that is of great importance to the health of society, the biosphere, and the climate.

Atmospheric
Chemistry
and Physics
Discussions

References

495

Baldwin, M. P., Gray, L. J., Dunkerton, T. J., Hamilton, K., Haynes, P. H., Randel, W. J., Holton, J. R., Alexander, M. J., Hirota, I., Horinouchi, T., Jones, D. B. A., Kinnersley, J. S., Marquardt, C., Sato, K., and Takahashi, M.: The quasi-biennial oscillation, Reviews of Geophysics, 39, 179–229, doi:10.1029/1999RG000073, 2001.

Ball, W. T., Haigh, J. D., Rozanov, E. V., Kuchar, A., Sukhodolov, T., Tummon, F., Shapiro, A. V., and Schmutz,
500   W.: High solar cycle spectral variations inconsistent with stratospheric ozone observations, Nature Geoscience, 9, 206–209, doi:10.1038/ngeo2640, 2016.

Ball, W. T., Alsing, J., Mortlock, D. J., Rozanov, E. V., Tummon, F., and Haigh, J. D.: Reconciling differences in stratospheric ozone composites, Atmospheric Chemistry & Physics, 17, 12 269–12 302, doi:10.5194/acp-17-12269-2017, 2017.

505   Ball, W. T., Alsing, J., Mortlock, D. J., Staehelin, J., Haigh, J. D., Peter, T., Tummon, F., Stuebi, R., Stenke, A., Anderson, J., Bourassa, A., Davis, S. M., Degenstein, D., Frith, S., Froidevaux, L., Roth, C., Sofieva, V., Wang, R., Wild, J., Yu, P., Ziemke, J. R., and Rozanov, E. V.: Evidence for a continuous decline in lower stratospheric ozone offsetting ozone layer recovery, Atmospheric Chemistry & Physics, 18, 1379–1394, doi:10.5194/acp-18-1379-2018, 2018.

510   Chipperfield, M. P., Bekki, S., Dhomse, S., Harris, N. R. P., Hassler, B., Hossaini, R., Steinbrecht, W., Thiéblemont, R., and Weber, M.: Detecting recovery of the stratospheric ozone layer, Nature, 549, 211–218, doi:10.1038/nature23681, 2017.

Chipperfield, M. P., Dhomse, S., Hossaini, R., Feng, W., Santee, M. L., Weber, M., Burrows, J. P., Wild, J. D., Loyola, D., and Coldewey-Egbers, M.: On the Cause of Recent Variations in Lower Stratospheric Ozone,
515   Geophys. Res. Lett., 45, 5718–5726, doi:10.1029/2018GL078071, 2018.

Choi, W., Lee, H., Grant, W. B., Park, J. H., Holton, J. R., Lee, K.-M., and Naujokat, B.: On the secondary meridional circulation associated with the quasi-biennial oscillation, Tellus Series B Chemical and Physical Meteorology B, 54, 395, doi:10.3402/tellusb.v54i4.16673, 2002.

Davis, S. M., Rosenlof, K. H., Hassler, B., Hurst, D. F., Read, W. G., Vömel, H., Selkirk, H., Fujiwara, M., and
520   Damadeo, R.: The Stratospheric Water and Ozone Satellite Homogenized (SWOOSH) database: a long-term database for climate studies, Earth System Science Data, 8, 461–490, doi:10.5194/essd-8-461-2016, 2016.

Dee, D. P., Uppala, S. M., Simmons, A. J., Berrisford, P., Poli, P., Kobayashi, S., Andrae, U., Balmaseda, M. A., Balsamo, G., Bauer, P., Bechtold, P., Beljaars, A. C. M., van de Berg, L., Bidlot, J., Bormann, N., Delsol, C., Dragani, R., Fuentes, M., Geer, A. J., Haimberger, L., Healy, S. B., Hersbach, H., Hólm, E. V.,
525   Isaksen, L., Kållberg, P., Köhler, M., Matricardi, M., McNally, A. P., Monge-Sanz, B. M., Morcrette, J.-J., Park, B.-K., Peubey, C., de Rosnay, P., Tavolato, C., Thépaut, J.-N., and Vitart, F.: The ERA-Interim reanalysis: configuration and performance of the data assimilation system, Quarterly Journal of the Royal Meteorological Society, 137, 553–597, doi:10.1002/qj.828, 2011.

Dhomse, S. S., Kinnison, D., Chipperfield, M. P., Salawitch, R. J., Cionni, I., Hegglin, M. I., Abraham, N. L.,
530   Akiyoshi, H., Archibald, A. T., Bednarz, E. M., Bekki, S., Braesicke, P., Butchart, N., Dameris, M., Deushi, M., Frith, S., Hardiman, S. C., Hassler, B., Horowitz, L. W., Hu, R.-M., Jöckel, P., Josse, B., Kirner, O., Kremser, S., Langematz, U., Lewis, J., Marchand, M., Lin, M., Mancini, E., Marécal, V., Michou, M., Morgenstern, O., O'Connor, F. M., Oman, L., Pitari, G., Plummer, D. A., Pyle, J. A., Revell, L. E., Rozanov, E., Schofield, R., Stenke, A., Stone, K., Sudo, K., Tilmes, S., Visioni, D., Yamashita, Y., and Zeng, G.: Es-

535   timates of ozone return dates from Chemistry-Climate Model Initiative simulations, Atmospheric Chemistry
        & Physics, 18, 8409–8438, doi:10.5194/acp-18-8409-2018, 2018.

Douglass, A. R., Stolarski, R. S., Strahan, S. E., and Oman, L. D.: Understanding differences in upper strato-
        spheric ozone response to changes in chlorine and temperature as computed using CCMVal-2 models, Journal
        of Geophysical Research (Atmospheres), 117, D16306, doi:10.1029/2012JD017483, 2012.

540   Douglass, A. R., Strahan, S. E., Oman, L. D., and Stolarski, R. S.: Understanding differences in chemistry
        climate model projections of stratospheric ozone, Journal of Geophysical Research (Atmospheres), 119,
        4922–4939, doi:10.1002/2013JD021159, 2014.

Dudok de Wit, T., Bruinsma, S., and Shibasaki, K.: Synoptic radio observations as proxies for upper atmosphere
        modelling, Journal of Space Weather and Space Climate, 4, A06, doi:10.1051/swsc/2014003, 2014.

545   Dunkerton, T. J. and Baldwin, M. P.: Quasi-biennial Modulation of Planetary-Wave Fluxes in the
        Northern Hemisphere Winter., Journal of Atmospheric Sciences, 48, 1043–1061, doi:10.1175/1520-
        0469(1991)048<1043:QBMOPW>2.0.CO;2, 1991.

Froidevaux, L., Anderson, J., Wang, H.-J., Fuller, R. A., Schwartz, M. J., Santee, M. L., Livesey, N. J.,
        Pumphrey, H. C., Bernath, P. F., Russell, III, J. M., and McCormick, M. P.: Global OZone Chemistry And
550   Related trace gas Data records for the Stratosphere (GOZCARDS): methodology and sample results with
        a focus on HCl, H_2O, and O_3, Atmospheric Chemistry & Physics, 15, 10 471–10 507, doi:10.5194/acp-15-
        10471-2015, 2015.

Froidevaux, L., Kinnison, D. E., Wang, R., Anderson, J., and Fuller, R. A.: Evaluation of CESM1 (WACCM)
        free-running and specified-dynamics atmospheric composition simulations using global multi-species satel-
555   lite data records, Atmos. Chem. Phys. Discuss., 15, 10 471–10 507, doi:10.5194/acp-2018-546, in review,
        2018.

Garfinkel, C. I., Gordon, A., Oman, L. D., Li, F., Davis, S., and Pawson, S.: Nonlinear response of tropical
        lower-stratospheric temperature and water vapor to ENSO, Atmospheric Chemistry & Physics, 18, 4597–
        4615, doi:10.5194/acp-18-4597-2018, 2018.

560   Gaudel, A., Cooper, O. R., and etc, E.: Tropospheric Ozone Assessment Report: Present-day distribution and
        trends of tropospheric ozone relevant to climate and global atmospheric chemistry model evaluation, Elem
        Sci Anth, 6, 10, doi:10.1525/elementa.291, 2018.

Harris, N. R. P., Hassler, B., Tummon, F., Bodeker, G. E., Hubert, D., Petropavlovskikh, I., Steinbrecht, W.,
        Anderson, J., Bhartia, P. K., Boone, C. D., Bourassa, A., Davis, S. M., Degenstein, D., Delcloo, A., Frith,
565   S. M., Froidevaux, L., Godin-Beekmann, S., Jones, N., Kurylo, M. J., Kyrölä, E., Laine, M., Leblanc, S. T.,
        Lambert, J.-C., Liley, B., Mahieu, E., Maycock, A., de Mazière, M., Parrish, A., Querel, R., Rosenlof, K. H.,
        Roth, C., Sioris, C., Staehelin, J., Stolarski, R. S., Stübi, R., Tamminen, J., Vigouroux, C., Walker, K. A.,
        Wang, H. J., Wild, J., and Zawodny, J. M.: Past changes in the vertical distribution of ozone - Part 3: Analysis
        and interpretation of trends, Atmospheric Chemistry & Physics, 15, 9965–9982, doi:10.5194/acp-15-9965-
570   2015, 2015.

Holton, J. R. and Tan, H.-C.: The Influence of the Equatorial Quasi-Biennial Oscillation on the
        Global Circulation at 50 mb., Journal of Atmospheric Sciences, 37, 2200–2208, doi:10.1175/1520-
        0469(1980)037<2200:TIOTEQ>2.0.CO;2, 1980.

Laine, M., Latva-Pukkila, N., and Kyrölä, E.: Analysing time-varying trends in stratospheric ozone time series using the state space approach, Atmospheric Chemistry & Physics, 14, 9707–9725, doi:10.5194/acp-14-9707-2014, 2014.

NCAR: The Climate Data Guide: Multivariate ENSO Index, Retrieved from https://climatedataguide.ucar.edu/climate-data/multivariate-enso-index, 2013.

Newman, P. A., Coy, L., Pawson, S., and Lait, L. R.: The anomalous change in the QBO in 2015-2016, Geophys. Res. Lett., 43, 8791–8797, doi:10.1002/2016GL070373, 2016.

Osprey, S. M., Butchart, N., Knight, J. R., Scaife, A. A., Hamilton, K., Anstey, J. A., Schenzinger, V., and Zhang, C.: An unexpected disruption of the atmospheric quasi-biennial oscillation, Science, 353, 1424–1427, doi:10.1126/science.aah4156, 2016.

Petropavlovskikh, I., Godin-Beekmann, S., Hubert, D., Damadeo, R., Hassler, B., and Sofieva, V.: SPARC/IO3C/GAW report on Long-term Ozone Trends and Uncertainties in the Stratosphere, SPARC/IO3C/GAW, SPARC Report No. 9, WCRP-17/2018, GAW Report No. 241, doi:10.17874/f899e57a20b, 2019.

Polvani, L. M., Sobel, A. H., and Waugh, D. W.: The Stratosphere: Dynamics, Transport, and Chemistry, Washington DC American Geophysical Union Geophysical Monograph Series, 190, doi:10.1029/GM190, 2010.

Polvani, L. M., Abalos, M., Garcia, R., Kinnison, D., and Randel, W. J.: Significant Weakening of Brewer-Dobson Circulation Trends Over the 21st Century as a Consequence of the Montreal Protocol, Geophys. Res. Lett., 45, 401–409, doi:10.1002/2017GL075345, 2018.

Randel, W. J., Wu, F., Swinbank, R., Nash, J., and O'Neill, A.: Global QBO Circulation Derived from UKMO Stratospheric Analyses., Journal of Atmospheric Sciences, 56, 457–474, doi:10.1175/1520-0469(1999)056<0457:GQCDFU>2.0.CO;2, 1999.

Slaper, H., Velders, G. J. M., Daniel, J. S., de Gruijl, F. R., and van der Leun, J. C.: Estimates of ozone depletion and skin cancer incidence to examine the Vienna Convention achievements, Nature, 384, 256–258, doi:10.1038/384256a0, 1996.

Solomon, S., Ivy, D. J., Kinnison, D., Mills, M. J., Neely, R. R., and Schmidt, A.: Emergence of healing in the Antarctic ozone layer, Science, 353, 269–274, doi:10.1126/science.aae0061, 2016.

SPARC/WMO: SPARC Report on the Evaluation of Chemistry-Climate Models, SPARC, 2010.

Steinbrecht, W., Froidevaux, L., Fuller, R., Wang, R., Anderson, J., Roth, C., Bourassa, A., Degenstein, D., Damadeo, R., Zawodny, J., Frith, S., McPeters, R., Bhartia, P., Wild, J., Long, C., Davis, S., Rosenlof, K., Sofieva, V., Walker, K., Rahpoe, N., Rozanov, A., Weber, M., Laeng, A., von Clarmann, T., Stiller, G., Kramarova, N., Godin-Beekmann, S., Leblanc, T., Querel, R., Swart, D., Boyd, I., Hocke, K., Kämpfer, N., Maillard Barras, E., Moreira, L., Nedoluha, G., Vigouroux, C., Blumenstock, T., Schneider, M., Garcìa, O., Jones, N., Mahieu, E., Smale, D., Kotkamp, M., Robinson, J., Petropavlovskikh, I., Harris, N., Hassler, B., Hubert, D., and Tummon, F.: An update on ozone profile trends for the period 2000 to 2016, Atmos. Chem. Phys. Discuss., 2017, 1–24, doi:10.5194/acp-2017-391, https://www.atmos-chem-phys-discuss.net/acp-2017-391/, 2017.

Stone, K. A., Solomon, S., and Kinnison, D. E.: On the Identification of Ozone Recovery, Geophys. Res. Lett., 45, 5158–5165, doi:10.1029/2018GL077955, 2018.

Strahan, S. E., Oman, L. D., Douglass, A. R., and Coy, L.: Modulation of Antarctic vortex composition by the quasi-biennial oscillation, Geophys. Res. Lett., 42, 4216–4223, doi:10.1002/2015GL063759, 2015.

615 Tachibana, Y., Inoue, Y., Komatsu, K. K., Nakamura, T., Honda, M., Ogata, K., and Yamazaki, K.: Interhemispheric Synchronization Between the AO and the AAO, Geophys. Res. Lett., 45, 13, doi:10.1029/2018GL081002, 2018.

Thomason, L., Ernest, N., Millan, L., Rieger, L., Bourassa, A., Vernier, J., Peter, T., Luo, B., and Arfeuille, F.: A global, space-based stratospheric aerosol climatology: 1979 to 2016, Earth Syst. Sci. Data, in preparation, 620 doi:10.5067/GloSSAC-L3-V1.0, 2017.

Tiao, G. C., Xu, D., Pedrick, J. H., Zhu, X., and Reinsel, G. C.: Effects of autocorrelation and temporal sampling schemes on estimates of trend and spatial correlation, Journal of Geophysical Research, 95, 20 507–20 517, doi:10.1029/JD095iD12p20507, 1990.

Toihir, A. M., Portafaix, T., Sivakumar, V., Bencherif, H., Pazmiño, A., and Bègue, N.: Variability and trend in 625 ozone over the southern tropics and subtropics, Annales Geophysicae, 36, 381–404, doi:10.5194/angeo-36-381-2018, 2018.

Tummon, F., Hassler, B., Harris, N. R. P., Staehelin, J., Steinbrecht, W., Anderson, J., Bodeker, G. E., Bourassa, A., Davis, S. M., Degenstein, D., Frith, S. M., Froidevaux, L., Kyrölä, E., Laine, M., Long, C., Penckwitt, A. A., Sioris, C. E., Rosenlof, K. H., Roth, C., Wang, H.-J., and Wild, J.: Intercomparison of vertically re- 630 solved merged satellite ozone data sets: interannual variability and long-term trends, Atmospheric Chemistry & Physics, 15, 3021–3043, doi:10.5194/acp-15-3021-2015, 2015.

Tweedy, O. V., Kramarova, N. A., Strahan, S. E., Newman, P. A., Coy, L., Randel, W. J., Park, M., Waugh, D. W., and Frith, S. M.: Response of trace gases to the disrupted 2015-2016 quasi-biennial oscillation, Atmospheric Chemistry & Physics, 17, 6813–6823, doi:10.5194/acp-17-6813-2017, 2017.

635 Wargan, K., Orbe, C., Pawson, S., Ziemke, J. R., Oman, L. D., Olsen, M. A., Coy, L., and Emma Knowland, K.: Recent Decline in Extratropical Lower Stratospheric Ozone Attributed to Circulation Changes, Geophys. Res. Lett., 45, 5166–5176, doi:10.1029/2018GL077406, 2018.

Weber, M., Coldewey-Egbers, M., Fioletov, V. E., Frith, S. M., Wild, J. D., Burrows, J. P., Long, C. S., and Loyola, D.: Total ozone trends from 1979 to 2016 derived from five merged observational datasets - the 640 emergence into ozone recovery, Atmos. Chem. Phys. Discuss., 2017.

WMO: Scientific Assessment of Ozone Depletion: 2014 Global Ozone Research and Monitoring Project Re- port, World Meteorological Organization, p. 416, geneva, Switzerland, 2014.

WMO: Scientific Assessment of Ozone Depletion: 2018, Global Ozone Research and Monitoring Project–Report, World Meteorological Organization, p. 588, geneva, Switzerland, 2018.

645 Zerefos, C., Kapsomenakis, J., Eleftheratos, K., Tourpali, K., Petropavlovskikh, I., Hubert, D., Godin-Beekmann, S., Steinbrecht, W., Frith, S., Sofieva, V., and Hassler, B.: Representativeness of single lidar stations for zonally averaged ozone profiles, their trends and attribution to proxies, Atmospheric Chemistry & Physics, 18, 6427–6440, doi:10.5194/acp-18-6427-2018, 2018.

Zerefos, C. S., Bais, A. F., Ziomas, I. C., and Bojkov, R. D.: On the relative importance of quasi-biennial 650 oscillation and El Nino/Southern Oscillation in the revised Dobson total ozone records, J. Geophys. Res., 97, 10, doi:10.1029/92JD00508, 1992.

Ziemke, J. R., Oman, L. D., Strode, S. A., Douglass, A. R., Olsen, M. A., McPeters, R. D., Bhartia, P. K., Froide-
vaux, L., Labow, G. J., Witte, J. C., Thompson, A. M., Haffner, D. P., Kramarova, N. A., Frith, S. M., Huang,
L.-K., Jaross, G. R., Seftor, C. J., Deland, M. T., and Taylor, S. L.: Trends in Global Tropospheric Ozone
655   Inferred from a Composite Record of TOMS/OMI/MLS/OMPS Satellite Measurements and the MERRA-2
GMI Simulation, Atmospheric Chemistry and Physics Discussions, 2018, 1–29, doi:10.5194/acp-2018-716,
https://www.atmos-chem-phys-discuss.net/acp-2018-716/, 2018.

Atmospheric
Chemistry
and Physics
Discussions
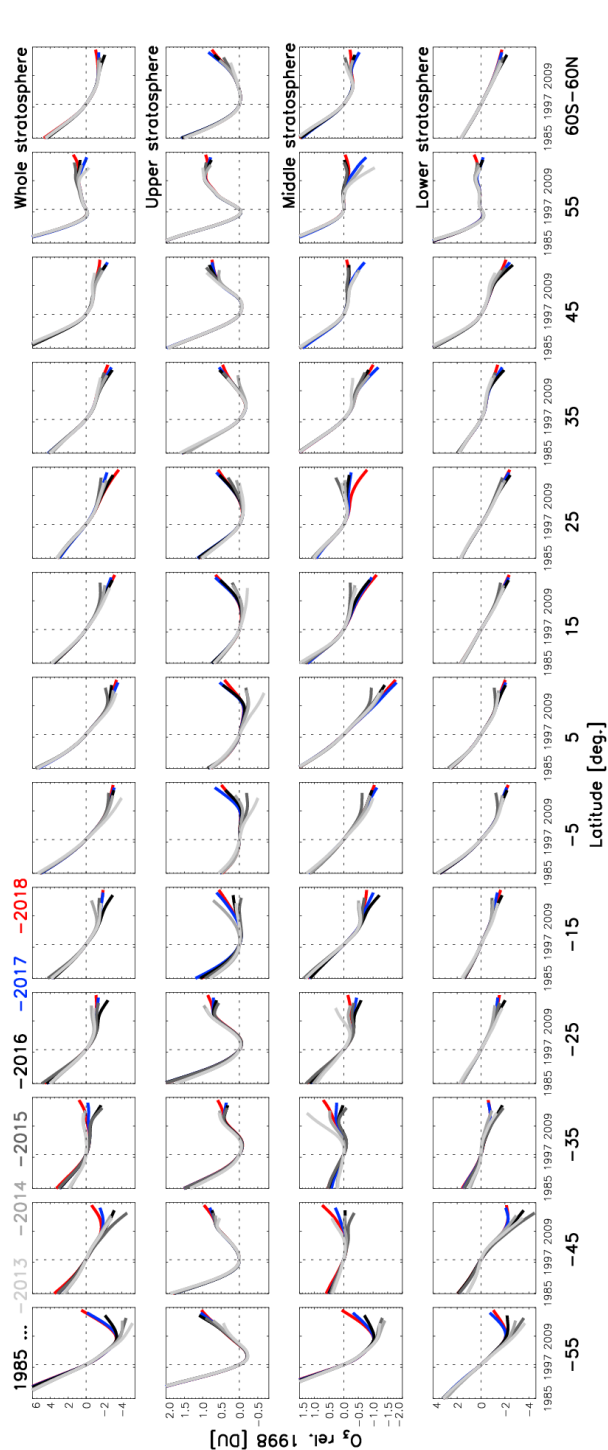
Figure 5: The partial column ozone non-linear trends estimated as a function of end year (2013 to 2018; dark to light colours), for each 10° latitude and quasi-global (left to right) and (top to bottom) the whole, upper, middle and lower stratosphere. Each sub-panel covers 1985–2018 and all curves are bias corrected to January 1998 (horizontal and vertical dotted lines). Uncertainties for each 1998–end-year change are given in Fig. 6.
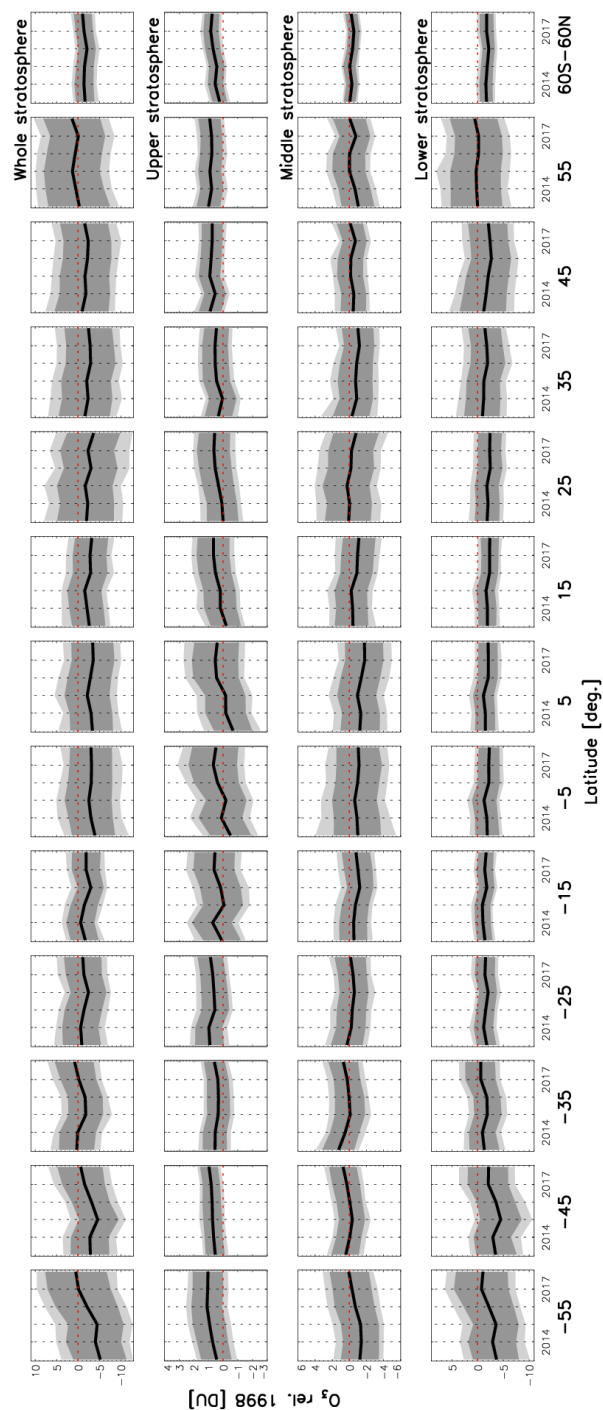
Atmospheric
Chemistry
and Physics
Discussions

Open Access

Figure 6: The partial column ozone changes between 1998 and the end-year from 2013 to 2018 (x-axis of each sub-panel) from the non-linear trends as in Fig. 5. Dark and light shading represent 95% and 99% credible intervals.
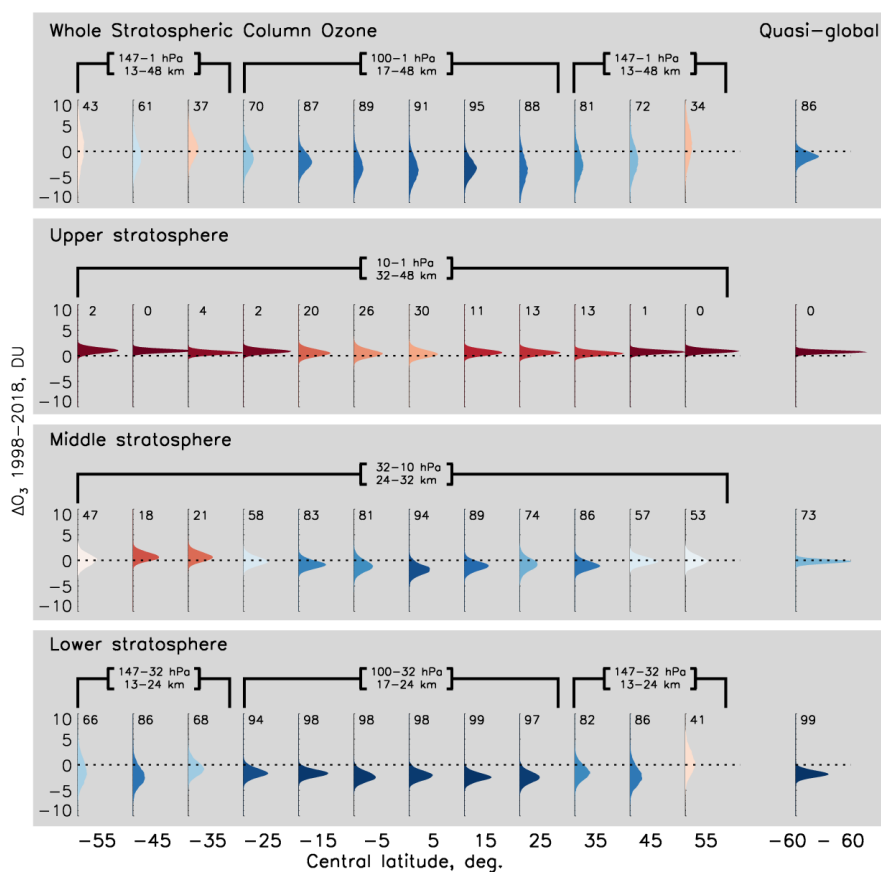
Figure 7: Posterior distributions (shaded) for the 1998–2018 partial column ozone changes. (Top) whole stratospheric column, (middle) upper and (bottom) lower stratosphere in 10° bands for all latitudes (left) and integrated from 60°S–60°N ('Global', right). The stratosphere extends deeper at mid-latitudes than equatorial (marked above each latitude). Numbers above each distribution represents the distribution-percentage that is negative; colours are graded relative to the percentage-distribution (positive, red-hues, with values <50; negative, blue).
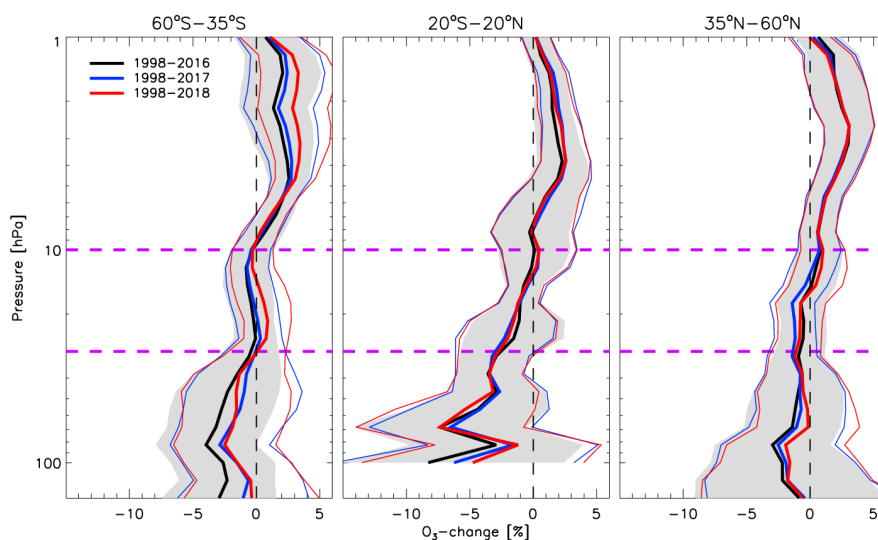
Figure 8: The ozone profiles for 1998 to an end-year of 2016 through 2018 (see legend) in the southern hemisphere (60°–35°S), the tropics (20°S–20°N), and the northern hemisphere (35°–60°N). Shading is for 2016 only. Uncertainties are 95% credible intervals. Pink lines indicate boundaries of partial columns in other figures.
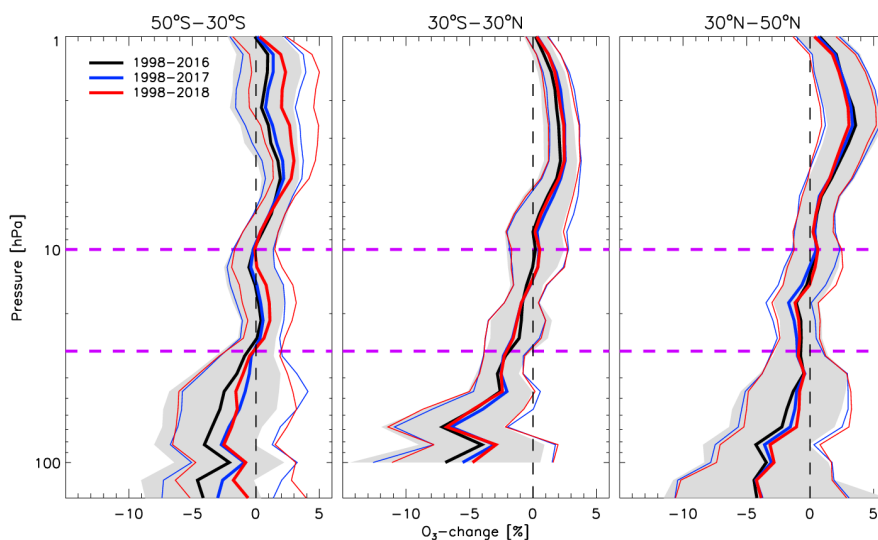

Figure 9: As for Fig. 8, but for the 50°S–30°S (SH), 30°S–30°N (tropics), 30°N–50°N (NH).